Design and Manufacturing of Lamb-Wave Biosensors Using PZT on SiN Thin Film

Jyh-Cheng Yu（余志成） and Jong-Xin Tsai
Department of Mechanical and Automation Engineering, National Kaohsiung First University of Science and Technology

Abstract

This study develops a Lamb-wave (Flexural Plate Wave, FPW) biosensing device using the structure of PZT thin film on Si_3N_4 membrane. A well-designed FPW device will have less energy dissipating into the sensing fluid and thus is suitable for biosensing. The sensitized film is coated on the membrane cavity, which can serve as the loading area of the sensing liquid. The material system of the device is Pt/Ti/PZT/LSMO/SiN/Si. The membrane for FPW is fabricated using KOH anisotropic etching. The PZT film (0.75 μm) is deposited using Sol-Gel technique. A thin film of LSMO will be added as the buffer layer between the PZT film and the electrodes to enhance the piezoelectric characteristics and the fatigue resistance. The total thickness of the composite plate is about 2 (μm). This paper presents the design of the biosensor and the manufacturing scheme. We have analyzed the effect of poling on the capacitance of IDTs. This study has successfully fabricated the Lamb wave device. The sensitized film has also been deposited on the membrane. The preliminary measurement result demonstrates the application feasibility of the Lamb wave biosensors.

***Keywords**:* Lamb wave, Flexural Plate Wave, Microsensor, PZT, Biosensor

1. Introduction

Lamb wave sensor is suitable for liquid sensing because of the low radiation loss if a slow mode of propagation, such as the lowest antisymmetric mode A_0, is excited. This type of Lamb wave sensor is also called the Flexural Plate Wave (FPW) sensor. The excitation and the detection of the acoustic waves are most readily accomplished by the use of interdigital transducers (IDTs) [1] on thin piezoelectric substrates. Toda [2] presented the equivalent circuit model for the delay line of FPW sensors, and suggested that the plate thickness should be smaller than 1/4 of the wavelength. The piezoelectric materials can be either crystal or thin films. The velocity of the acoustic waves is very sensitive to the properties of the propagating surface. If the surface of the propagating substrate is disturbed by external measurands such as mass loading, damping, and mechanical loading, the resonant frequency will shift accordingly.

Piezoelectric thin films have the cost advantage over crystal materials. Most Lamb wave devices of piezoelectric thin films employ zinc oxide (ZnO) [14][15] and aluminum nitride (AlN) [16]. The application of Lead Zirconate Titanates (PZT) thin films is very promising because the electromechanical coupling coefficient (K^2) of is three to nine times over AlN and ZnO, which can greatly improve the sensitivity of sensing devices.

Many studies apply FPW sensors to liquid sensing. Costello etc. [3] proposed a FPW device using ZnO for viscosity sensing. The experimental result showed that the insertion loss increases and the resonant frequency reduced with the increase of the liquid viscosity. Weinberg etc. [4] derived the fluid damping model of the FPW device with AlN and compared with the experiment results. On the other hand, Lugunbuhl etc. [5] adopted the sol-gel derived PZT thin film in the FPW device, and showed that the resonant frequency will reduce and the insertion loss will increase as the thin film is loaded with DI water. The study also indicated that the poling of PZT film would reduce the insertion loss.

FPW devices can be applied to biosensing when the sensing area of a delay line is coated with a bio-sensitized film. Pyun etc. [6] deposited an immunoaffinity layer on the membrane of the FPW device to detect Escherichia Coli (E. Coli). The gravimetric detection limit is less than 6 (ng) at a 32 (μm) thick sensitive layer in aqueous media. Kondoh etc. [7] detected urease using SH-SAW propagating on the $LiTaO_3$ substrate. Many bacteria contain urease and will generate ammonia that will change the pH value of the solution. The velocity of SH-SAW is very sensitive to the pH value of the loading liquid. Therefore, the concentration of bacteria can be detected by the change of the wave velocity. Campitelli etc. [8] fixed Protein A on a SH-SAW device to detect the concentration of Immunoglobulin G (IgG) by the selective bonding between IgG and Protein A. Besides, SAM, SAv molecule and Biotin-BSA molecule have the high bonding characteristic, which can be used to detect the weight of Biotin-BSA and Anti-BSA molecules [9].

This paper adopts a Lamb-wave biosensing device using the structure of sol-gel derived PZT thin film on Si_3N_4 membrane. A thin film of LSMO will be added as the buffer layer between the PZT film and the electrodes to enhance the piezoelectric characteristics and the

* jcyu@ccms.nkfust.edu.tw

fatigue resistance. This study will investigate the complete development procedure of the proposed biosensing component from the device design and fabrication, the PZT thin film deposition, the immobilization of antibody, and the preliminary signal analysis.

2. The Fabrication Procedure

The device is fabricated using planar processes and anisotropic etching. The material system of the device consists of Pt /Ti /PZT (0.75 μm)/LSMO/SiN (1.2 μm)/Si. The fabrication sequences is illustrated in Fig. 1. Starting from a (100) silicon substrate, the composite acoustic membranes were fabricated by LPCVD silicon nitride, a (La_xSr_{1-x}) MnO_3 (LSMO) layer, and multi-layers of sol-gel-derived PZT. The pattern of back cavity is defined by lithography. RIE is used to pattern SiN for the masking layer of backside etching. The LSMO layer is used as a buffer layer between the PZT and SiN, which can enhance the piezoelectric characteristic. Composite metal films consisted of Pt and Ti is patterned using lift-off techniques. The function of Ti serves as an adhesion layer between Pt and PZT, and avoids possible diffusion. The membrane cavity of the device is fabricated using KOH (30 wt% and 80 °C) anisotropic etching. Finally, we deposit Cr and Au as adhesion layers to coat the bio-sensitized film.

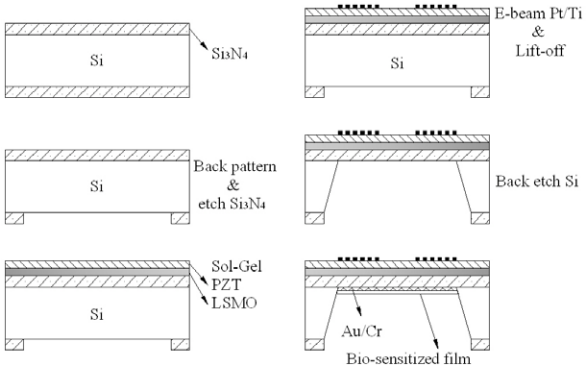

Fig. 1 The fabricating procedure of the biosensor

3. The Design of the Lamb Wave Device

3.1. The Delta Function Modeling of IDT

The Lamb wave device adopts the structure of the IDT delay line, which is a two-port design. The stimulus, such as mass loading and fluid damping, on the conducting plate will incur the velocity change. The period of the IDTs determines the acoustic wavelength. Thus, the velocity change of Lamb wave can be picked up as frequency shift using on oscillator set-up.

The delay line device includes an input and an output IDTs and a delay region. The frequency response diagram is as Fig. 2, where $H_i(f)$ and $H_o(f)$ represent the frequency response of the input and the output IDTs respectively, $e^{-j\beta x(f)}$ represents the phase delay between input and output IDTs, $\beta=2\pi/\lambda$ is the phase constant, and $x(f)$ is a frequency-dependent separation between those segments of input and output IDTs. When the input and output IDTs have a uniform finger separation as well as uniform finger apodization overlap, $x(f) = L$, L is the distance between the midpoint of the bi-directional input and output IDTs.

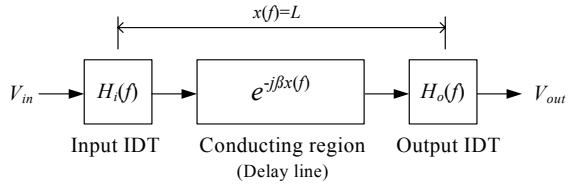

Fig. 2 The frequency response block diagram

The preceding relations are applied to obtain $H_1(f)$ for the input IDT. The frequency response $H_2(f)$ of the output IDT is obtained in the same way. Its relative phase shift will also be just 0° or 180°, because the imaginary parts cancel out in summation. Therefore $H_1(f)$ is entirely in terms of the real quantity $\cos(\beta x)$. When the IDT is excited, the surface wave will flow outward in both directions along the propagation direction. Thus the inherent loss of the IDT will be 3 (dB), which induces a least 6 (dB) difference between the input and the output signals. In the following simulation, we consider only the relative loss for the IDT design.

Taking the single-electrode IDT as an example, the electrode fingers alternate in voltage polarity with centers spaced $\lambda_0/2$. Given the metallization ratio $\eta=1/2$, the wavelength (λ_0) of the excited waves is $4d$ where d is the width of the electrode. The delta-function model of single-electrode IDT is as follows:

$$H_{i1}(f) \cong \left[\frac{\sin\left[N_p\pi(f-f_0)/f_0\right]}{N_p\pi(f-f_0)/f_0}\right] = \mathrm{sinc}\left[N_p\pi(f-f_0)/f_0\right] \quad (1)$$

where N is the number of the IDT fingers, f0 is the resonant frequency, Np represents the number of positive electrodes of the single-electrode IDT, and Np=N/2. Given the phase velocity of the acoustic wave vp, the resonant frequency f0 is equal to vp/λ0. The model is close to a sinc function as shown in Eq.(1) if Np is large.

Following the similar procedure, the IDT model with the design of split-electrode, $H_{i2}(f)$ can be expressed as follows:

$$H_{i2}(f) \cong 2\cos\left(\frac{\pi f}{4f_0}\right)\times\mathrm{sinc}\left[N_p\pi(f-f_0)/f_0\right] \quad (2)$$

where $H_{i2}(f)$ is the transfer function of the split-electrode IDT and $N_p=N/4$ is the number of pairs of the positive electrodes in the split-electrode IDT.

3.2. The Simulation Results

The Delta-function model is close to a *sinc* function for a large N_p. The first null of the frequency response will happen in $\sin[N_p\pi(f-f_0)/f_0]= \sin(n\pi)$ that also can be derived that $BW_{nn}= 2f_0/N_p$, where BW_{nn} is the bandwidth of the first null relative to both sides of the center.

Fig. 3 shows that difference of the simulating conditions for $\lambda_1=\lambda_2$ ($d_1=2d_2$, $f_1=f_2$) and $N_{p1}=N_{p2}=20$, where the suffix "1" and "2" represent the single-electrode and the split-electrode IDTs. We can observe that the peak of the split-electrode IDT is sharper than the single-electrode, and the sidelobes of the split-electrode is smaller as well. These two designs will have the same bandwidth if the IDT period and N_p are the same. However, the split design will have twice the number of electrodes compared with the single-electrode design.

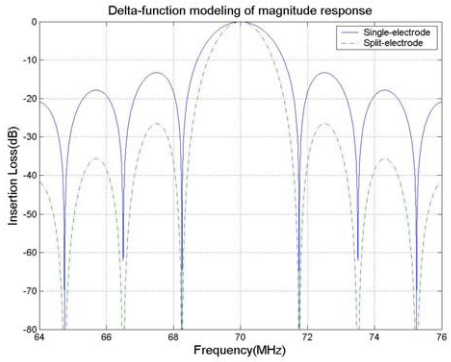

Fig. 3 The frequency response diagram for single and split IDT designs ($\lambda_1=\lambda_2$, N_p=20)

3.3. The phase velocity of the flexural plate wave

The velocity of Lamb wave is determined by the thickness, the mechanical properties, and the boundary the conditions of the conducting composite plate. Therefore, the thin plate can serve as a transducer. The phase velocity of the thin-plate regime can be well approximated by the simple asymptotic expression [10]:

$$v_P = \left(\frac{B + T_x}{M}\right)^{1/2} \tag{3}$$

where B is the bending stiffness of a homogeneous, elastically isotropic plate, T_x is the component of in-plane tension in the propagation direction, and M is the mass per unit area of the plate. For an A_0 Lamb wave in a tension-free plate, the bending stiffness takes the from

$$B = \left(\frac{\lambda}{2\pi}\right)^2 \frac{E' d^3}{12} \tag{4}$$

E' is the effective Young's modulus:

$$E' = \frac{E}{1-\nu^2} \tag{5}$$

where E is the Young's modulus and ν is the Poisson's ratio of the material.

3.4. Gravimetric detection of an added mass in a liquid:

The device can be applied to a biosensor that may detect the adsorption or attachment of a layer of particular molecules on the sensing region. The phase velocity of the device can be expressed as below:

$$v_P \cong \left(\frac{T_x + B}{M + \rho_F\delta_E + m_{sorptive} + \Delta m}\right)^{1/2} \tag{6}$$

where $\rho_F\delta_E$ is the equivalent loading of the liquid; $m_{sorptive}$ is the mass per unit area of any selective biological or chemically sorptive layer, and Δm is the detectable added mass per unit area. In this study, $m_{sorptive}$ and Δm can be considered as the antibody layer and the locked-in antigen. The equivalent thickness of the liquid loading is as follow:

$$\delta_E = \left(\frac{\lambda}{2\pi}\right)\left[\left(1-\frac{v_P}{v_F}\right)^2\right]^{-1/2} \tag{7}$$

where v_F is the acoustic velocity of the loading liquid. For plates and fluids that satisfy $v_p<<v_F$, the term in the brackets is approximately unity.

$$\delta_E \cong \frac{\lambda}{2\pi} \tag{8}$$

When the loading liquid is dripped on the thin plate, if the contacting surface is not hydrophilic, the droplet will not spread out and remain hemispherical as shown in Fig. 4. Because of the evanescent decay length is approximate $\lambda/2\pi$, not all the mass of the loading drop will contribute the mass loading effect. Because the shape of the drop can't be accurately controlled, the change of the phase velocity usually is not in proportional to the number of liquid drops. Therefore, this device is more suitable to detect the liquid density when the loading liquid is filled in the cavity of the sensing region.

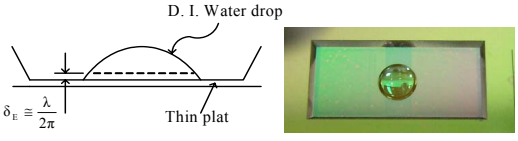

Fig. 4 The evanescent decay length of acoustic waves

Equation (6) shows that the phase velocity of FPW biosensors will be influenced by the coupling effects of (1) the mass effect ($\rho_F\delta_E$) caused by the loading liquid, (2) the added mass effect (Δm) due to the absorbed

antigen, and (3) the tension effect (T_x) caused by the liquid pressure.

$$\frac{\Delta v_p}{v_p} = s_m \times (\rho_F \delta_E + m_{sorptive} + \Delta m) + s_T \times T_x \quad (9)$$

This study proposes the sensor design that consists of two Lamb wave devices as illustrated in Fig. 5. The first one is applied to detect external perturbation and the other one is filled with the reference solution. When the heights of both liquids exceed the evanescent decay length, the mass loading will be the same. The liquid pressure will be the same as well. Here, the comparison of the two devices can isolate the effect of added mass due to antigen bonding and compensates unnecessary perturbation.

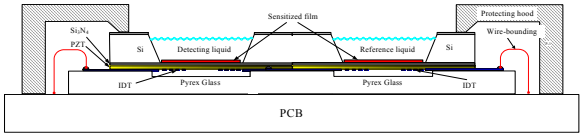

Fig. 5 The diagram of the device

3.5. The estimated sensitivity and the phase velocity of the device

For such a device the gravimetric sensitivity is

$$s_m = -\frac{1}{2\left(M + \rho_F \delta_E + m_{sorptive}\right)} \quad (10)$$

We then find that the minimum detectable added mass, $\Delta m_{\min}$, in this fluid-loaded case with a sorptive film is just

$$\Delta m_{\min} = \frac{1}{s_m}\left(\frac{\Delta f_{\min}}{f}\right) \quad (11)$$

where $\Delta f_{\min}$ is the minimum significant frequency shift.

The structure of the proposed device is Pt/Ti/PZT(0.75 μm)/LSMO(0.1 μm)/SiN(1.2 μm)/Si/Ti/Au(0.2 μm). Table. 1 lists the mechanical properties of the composite plate [11]~[13]. Here, we assume (1) the characteristic of the LSMO film is the same as the PZT film, and (2) the thickness of the adhesion layer Cr is negligible.

Table. 1 The parameters of the plate

	Si_3N_4	PZT (PZT + LSMO)	Au
Thickness (μm)	1.2	0.85 (0.75+0.1)	0.2
Young's modulus (E, N/m^2)	$3.85*10^{11}$	$4*10^{10}$	$0.8*10^{11}$
Poisson ratio (υ)	0.27	0.3	0.33
Density (ρ, kg/m^3)	3100	7550	19300
M (kg/m^2)	0.00347	0.00642	0.00386

Table. 2 the parameters of the composite plate

E	$7.805*10^{10}$ (N/m^2)
M	0.0969 (N/m^2)
v	0.282
E'	$8.479*10^{10}$ (N/m^2)

The thickness of the composite plate is 1.2+0.85=2.05 (μm) Table. 2 are the estimated parameters of the composite plate.

The wavelength of the proposed sensor is 80 (μm). The bending stiffness of the plate can be calculated as 375.49 (N/m). Therefore, the phase velocity of the device without liquid loading $v_{p(\text{air})}$ = 62.249 (m/s) and the resonant frequency:

f_{air} = 0.778 (MHz).

The velocity of water is about 1480 (m/s), and $v_{p(\text{air})}$ is 62.249 (m/s). Then $v_p << v_f$,

$$\delta_E \cong \frac{\lambda}{2\pi} = \frac{80}{2\pi} = 12.732(\mu\text{m})$$

The mass loading effect is as follows:

$\rho_F \delta_E$ = 0.1249 (N/m^2)

The tension effect due to the liquid weight is negligible compared with the bending stiffness of the plate.

$$v_P \cong \left(\frac{T_x + B}{M + \rho_F \delta_E}\right)^{1/2} = 41.145(\text{m/s})$$

$$f_{water} = \frac{v_p}{\lambda} = \frac{41.145}{80} = 0.514(\text{MHz})$$

Assuming the minimum differentiable frequency shift is 10 (Hz), We can estimate the sensitivity of the device is –170.1 (cm^2/g). Therefore, the minimum mass change, $\Delta m_{\min}$ could be detected and examined is approximately $0.113*10^{-10}$ (g/cm^2). Equation (10) shows that the mass loading part $\rho_F \delta_E$ has a great influence on the sensitivity, where $\delta_E = \lambda/2\pi$. When the design of wavelength is smaller, the s_m can be increased.

4. Experimental Results and Discussions

4.1. The parallel poling of the PZT films with IDT

Because PZT is polycrystalline, polarization using DC poling will increase the net capacitance of the transducer. There are three main factors influencing the poling result including poling time, poling voltage, and substrate temperature. We use the LCR meter to measuring the (C_s).

Fig. 6 shows the measured capacitance of IDT using the poling voltage from 10(V) to 50(V) at substrate temperature of 250(°C) for three hours. The capacitance increases significantly with the applied poling voltage. When the applied voltage exceeds 40(V), the increase of the capacitance becomes saturate.

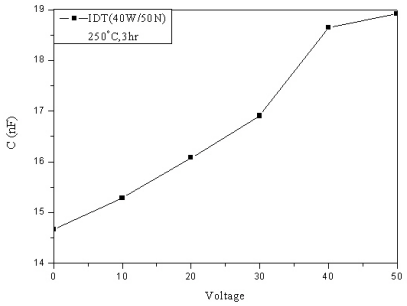

Fig. 6 The relation between the IDT capacitance and the poling voltage at 250 °C for 3hr.

Fig. 7 shows that the effect of the heating temperature in the poling process. The poling voltage is set as 40 V for 3 hr as suggested from the previous experiment. Again, the capacitance increasing saturates when the poling temperature reaches 250(°C).

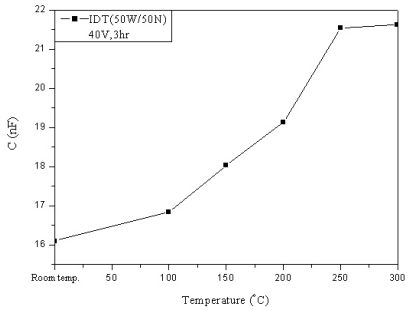

Fig. 7 The relation between the IDT capacitance and the substrate temperature at the DC poling of 40V for 3hr.

4.2. The deposition of the bio-sensitized film

The bio-sensitized film is deposited on the cavity side of the membrane. The first step is to deposit A Au/Ti adhesion layer is used between the antibody layer and the SiN membrane. The depositing result is examined using immuofluorescence as illustrated in Fig. 8. When the antibodies is successfully fixed on the membrane, which will show a The luminous points shows that the antibody layer is successfully coated on the membrane area.

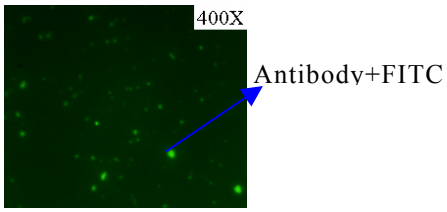

Fig. 8 The coating of the bio-sensitized film

4.3. SAW and FPW signals

Before the anisotropic etching of the silicon substrate, the IDT will excite Raleigh waves because of the semi-infinite substrate. We measure the SAW signal to verify the design. The wavelength of the IDT design is 80 (μm). As depicted in the frequency response of S_{21} transmission coefficient in Fig. 9, the frequency of the Raleigh wave is around 63 MHz.

The membrane cavity is then fabricated using KOH etching. The concentration of the KOH solution is 30 % and the temperature is 80 °C. The final composite membrane consists of 1.2(μm) silicon nitride, 0.1(μm) LSMO, and 0.75(μm) PZT. From the measurement result shown in Fig. 10, the frequency of the Lamb wave is around 0.46 (MHz) that is close to the analytical result in section 3.5.

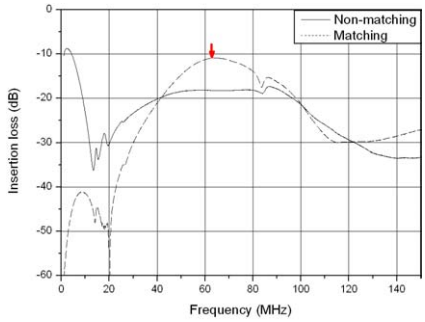

Fig. 9 The frequency response of SAW

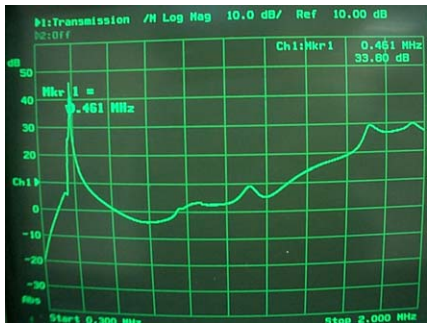

Fig. 10 The frequency response of FPW

5. Conclusions

This study has described the design and the fabrication procedure of the proposed Lamb wave device using the PZT on SiN structure. The sol-gel derived PZT film demonstrates promising characteristics in the application of the DC poling. We have successfully fabricated the Lamb wave device and coated the sensitized layer on the membrane. The preliminary measurement result demonstrates the application feasibility of the Lamb wave biosensors.

6. Acknowledgment

The authors world like to thank the National Science Council of the Republic of China for financially supporting this research under Contract No. NSC 93-2216-E-327-001

7. References

1. White, R. M. and Voltmer, F. M. “Direct piezoelectric coupling to surface elastic waves”, *Appl. Phys. Lett*., Vlo. 7, pp. 314-316, 1965
2. Toda, K., “Lamb-wave delay lines with Interdigital electrodes”, *Japanese Journal of Applied Physics*, Vol. 44, pp. 56-62, 1973.
3. Costello, B. J. “Ultrasonic Plate Waves for Biochemical Measurements”, *Ultrasonics Symposium*, pp. 977-981, 1989.
4. Weinberg, Marc S. “Fluid Damping in Resonant Flexural Plate Wave Device”, *Journal of Microelectromechanical Systems*, Vol. 12, No. 5, pp. 567-576, 2003.
5. Luginbuhl, P., “Microfabricated Lamb Wave Device Based on PZT Sol-Gel Thin Film for Mechanical Transport of Solid Particles and Liquids”, *Journal of Microelectromechanical Systems*, Vol. 6, No. 4, pp. 337-346, 1997.
6. Pyun, J.C., Beutel, H., Meyer, J.-U., and Ruf, H.H. “Development of a biosensor for E. coli based on a flexural plate wave (FPW) transducer”, *Biosensors & Bioelectronics*, v 13, n 7-8, pp. 839-845, Oct 1, 1998.
7. Kondoh, J, Matsui, Y, and Shiokawa, S., “SH-SAW biosensor based on pH change”, *IEEE Ultrasonics Symposium Proceedings*. vol.1, pp.337-340, 1993.
8. Campitelli, A., Wlodarski, W., Hoummady, M., and Sawyer, W., “Shear horizontal surface acoustic wave based immunosensing system”, *Solid State Sensors and Actuators. TRANSDUCERS '97* Chicago., 1997.
9. White, R. M., “Acoustic sensors for physical, chemical and biochemical applications”, *IEEE Frequency Control Symposium*, pp. 587-594, 1998.
10. Campbell C. *Surface acoustic wave devices for mobile and wireless communications*, Academic Pr, 1998.
11. Tjhen, W., Tamagawa, T., Ye, C.-P., Hsueh, C.-C., Schiller, P., and Polla, D.L. “An Investigation of Micro Structures, Sensors, Actuators, Machines and Robots”, *IEEE Micro Electro Mechanical Systems*, pp. 114-119, 1991.
12. Yu, J. and Lan, C., “System Modeling and Robust Design of Microaccelerometer Using Piezoelectric Thin Film”, *Proceedings of the 1999 IEEE International Conference on Multisensor Fusion and Integration for Intelligent Systems*, Taipei, ROC., pp. 99-104, 1999.
13. Rashidian, B. and Allen, M.G., “Electrothermal microactuators based on dielectric loss heating”, *IEEE Actuators, Machines and Systems*, pp. 24-29, 1993.
14. Vellekoop, M.J., Lubking, G.W., Sarro, P.M., and Venema, A. “Evaluation of liquid properties using a silicon lamb wave sensor”, *Sensors and Actuators A*, 43, pp.175-180, 1994.
15. Wenzel, S. W. and White, R.M., “A Multisensor Employing an Ultrasonic Lamb-Wave Oscillator”, *IEEE Transactions on Electron Devices*, Vol.35, No.6, pp.735-743, June 1988.
16. Choujaa, A., Tirole, N., Bonjour, C., Martin, G., Hauden, D., Blind, P., Cachard, A., and Pommier, C. “AlN/silicon lamb wave microsensors for pressure and gravimetric measurements”, *Sensors and Actuators A*, Vol. 46, pp. 179-182, 1995.

結合鋯鈦酸鉛與氮化矽薄膜於蘭姆波生物微感測元件之設計與製造

余志成　蔡宗欣
國立高雄第一科技大學機械與自動化工程系

摘要

本論文研究以PZT壓電薄膜激震之平板聲波元件作為生醫感測之元件架構。平板波(Flexural Plate Wave)/蘭姆波(Lamb Wave)因不易受到待測液體的波傳能量散射，且其背蝕刻所造成薄膜孔穴，適合用來鍍製生化感測元件中的敏感層，作為液體感測。本研究的元件材料結構採用超聲波於壓電薄膜與氮化矽(piezoelectric thin film on silicon nitride)，整個材料系統為 Pt/Ti/PZT/LSMO/Si_3N_4/Si，聲波傳遞薄膜以1.2(μm)氮化矽薄膜，經由KOH非等向性蝕刻而成。壓電薄膜採用溶膠凝膠法進行退火處理之鋯鈦酸鉛(PZT)薄膜(約0.75μm)，並輔以氧化物電極作為IDT的材料系統，藉以提升薄膜電性與疲勞特性。本研究完成了生醫元件設計與製程的規劃，並探討PZT壓電薄膜極化方式對指叉電容的影響，已研製出蘭姆波感測元件，並量測出基本的訊號響應。而生化感測薄膜也成功的鍍製於感測區薄膜，驗證了本元件應用於生醫感測的可行性。

關鍵字：蘭姆波、平板波、生物微感測器、鋯鈦酸鉛、壓電薄膜